Effect of Additives on Self-Assembling Behavior of Nafion in Aqueous Media

Suhong Jiang,[†] Ke-Qing Xia,*[,†] and Gu Xu[‡,§]

Department of Physics, The Chinese University of Hong Kong, Hong Kong, China; Department of Materials Science & Engineering, McMaster University, Hamilton, Canada L8S 4L7; and Department of Materials Science, National University of Singapore, Singapore 119260

Received January 22, 2001; Revised Manuscript Received July 19, 2001

ABSTRACT: The dynamic light scattering technique is employed to study the self-assembling behavior of Nafion in dilute aqueous solutions and in water-based mixture solvents. The mixture solvents contain either salt or a small amount of glycerol, which is often necessary for the fabrication of the electrode−membrane assembly. Two kinds of aggregates are found in Nafion aqueous solutions: (1) an intrinsic aggregate (∼150 nm) due to the hydrophobic interaction of fluorocarbon backbone, which is found to be always present in aqueous solutions; (2) a larger, secondary aggregate, which can be suppressed by the addition of salt or a small amount of glycerol. This secondary/higher level aggregation may arise from the electrostatic attraction through the nonionized ion pairs, which are believed to facilitate the formation of large ion clusters and provide the ion connection between the ion clusters. We discuss the structures of Nafion aggregates based on the rodlike microstructure units and propose a microgel-type aggregation model.

Introduction

As the first commercially available perfluorosulfonated ionomer (PFSI), Nafion has been extensively used in the recent development of proton-exchange membrane fuel cells (PEMFC) for future electric automobiles.[1−5] It possesses unique properties, such as high permeability to water and cationic species and excellent mechanical, chemical, and thermal stabilities. Initially, Nafion's main application was in the electrochemical industry. But beginning from the mid-1980s, it has become an "indispensable" part for the polymer fuel cell research and electric vehicle development, largely in response to the more stringent call for a cleaner environment. Besides its application as the proton-exchange membrane (PEM), the core part of a fuel cell to separate the fuel and the oxidant, Nafion is also used in solution form for casting into the electrode−membrane assembly (EMA), because a fuel cell electrode transports both ions and electrons.[4,5] One serious problem, however, occurs from time to time when Nafion is dissolved and recast into a membrane; its ionic conductivity drops by up to 4 orders of magnitude.[6] The same thing happens when a small amount of glycerol is used in the solution casting; the addition of glycerol is often necessary for the adhesion of the EMA onto the substrate. This reduces tremendously the fuel cell efficiency and limits its overall performance.

Prior to the discovery of this problem for the recast membranes, the structure of "as-received" Nafion membranes had been extensively studied by various methods.[7−11] For example, in an effort to identify the morphology, wide-angle X-ray diffraction indicates that there is, at least, partial crystallinity in Nafion, as evidenced by the Bragg peak superimposed on an amorphous background.[7−10] It has also been demonstrated that the degree of the crystallinity decreases with decreasing equivalent weight (EW) due to the increasing concentration of the side-chain material. Moreover, small-angle X-ray scattering reveals that there exist ion-rich domains or "clusters".[7,10] It has been proposed that these clusters, containing the majority of the ion pairs, act as multifunctional "electrostatic" cross-links due to their strong Coulombic nature.[11] In the meantime, these ionic clusters produce very high ionic conductivities, even comparable to the liquid electrolytes, and almost perfect cationic transference number.[12,13] However, none of these are maintained after the membrane is high temperature dissolved,[6] the only way to physically decompose the membrane.[10,14,15] The recast membranes not only have a much-reduced cationic conductivity but also absorb much less amount of water, a strong indication of underdeveloped or even suppressed ionic clusters.[6] The same decrease in ionic conductivity has been observed from the membranes cast from the solution form of Nafion, which has been added with a small amount of glycerol, a necessary agent for the EMA. Although the ion conductivity can be improved by certain additives, such as moisture-absorbing reagents, organic sulfonate compounds, and structure aligning copolymers with ion-exchange sites,[16] they affect negatively the chemical and thermal stabilities.

Recently, the Nafion solution and the membrane casting process have received increasing attention.[17,18] The self-assembling of the Nafion chains in water, methanol (MeOH), ethanol (EtOH), triethyl phosphate (TEP), formamide (FA), *N*-methylformamide (NMF), *N*,*N*-dimethylformamide (DMF), and *N*,*N*-dimethylacetamide (DMA) solutions have been studied by small-angle neutron and X-ray scattering (SANS and SAXS, respectively).[19,20] Similar studies have also been carried out on the short pendant chain perfluorinated ionomer (SPC PFSI) solutions.[21] Rodlike structures, which are arranged in planar hexagonal array or mutually orthogonal rods, are observed in all Nafion solutions and

† The Chinese University of Hong Kong.
‡ McMaster University.
§ National University of Singapore.
* To whom correspondence should be addressed.

10.1021/ma010124b CCC: $20.00
Published on Web 09/27/2001

SPC PFSI solutions in all of the solvents. In these structures, the perfluoro backbones constitute the solvophobic core of the rods, and the ionic groups sit at the rod−solvent interface. Electron spin resonance (ESR) spectra of spin probes reveal certain structural details of self-assembling in PFSI aqueous solutions[22,23] and nonaqueous solutions.[24] These ESR studies showed the existence of aggregation in aqueous solutions and most of the nonaqueous solution.

Nafion solutions are interesting also from the point of view of ionomer solution studies. Ionomer solutions can be classified into three types: (i) ionomer solutions in nonpolar solvents are characterized by a concentration-dependent equilibrium between intra- and interchain aggregation owing to the electrostatic attraction between nonionized ion pairs on the solvated backbone; (ii) ionomer solutions in polar solvents that are able to dissolve the polymer backbone are characterized by rather extended polymer chains similar to weakly charged polyelectrolytes; and (iii) ionomer solutions in polar solvents in which the analogous neutral polymer is not soluble are characterized by polymer−solvent phase separation, leading to a colloidal dispersion. The particles are expected to constitute a polymer core with the ionic groups at the polymer−solvent interface. While many systems belong to the first two categories, a few systems belong to the third, which includes the PFSI and polyethylene-*co*-methacylate aqueous solutions.[25] Although, the microstructure of PFSI solutions has been extensively studied using X-ray and neutron scattering techniques, the aggregation form of Nafion solutions is not completely understood.

In this paper, we report studies of the aggregating structures of Nafion solutions. Dynamic light scattering (DLS) is chosen for its power of elucidating the motion of polymer aggregates down to nanometer scales.[26,27] A similar paper was published by Cirkel et al. using dissolved Nafion film.[28] To rule out the possible residual structures from the solid state, a more detailed job was therefore planned to investigate the phenomena using liquid Nafion. In the meantime, a very strict cleaning procedure, including the solvent filtering by 200 nm pore, was followed to eliminate possible contamination of the sample solution. Moreover, we would like to vary sample concentration and verify the q^2 dependence by a full angular range. Finally, we would also like to investigate the effects of adding small amount of salt and glycerol into the Nafion aqueous solutions.

Experimental Section

Materials. Nafion is a commercially available perfluorosulfonated ionomer (PFSI), with a chemical formula of $-[C(-R)F-CF_2-(CF_2-CF_2)_n]_m-$, where R = $-O-CF_2-CF(CF_3)-O-CF_2-CF_2-SO_3-M^+$ and M^+ is the counterion or H^+. The 5 wt % water/ethanol (EtOH) Nafion solution used in this study was purchased from du Pont. Other chemicals, including absolute ethanol (CH_3CH_2OH), glycerol [$HOCH_2CH(OH)-CH_2OH$], and LiCl, were all reagent grade commercial products and were used as received without further purification.

Sample Preparation. 5 mL of 5% Nafion water/EtOH (1:1) solution was mixed with 50 mL of deionized water. The mixture was then heated at 70 °C to evaporate most of the solvent until about 5 mL was left. All of the dilute solutions of Nafion in water or in water-based solvents (5% glycerol, 0.5 M LiCl) were prepared by dilution of this concentrated stock Nafion aqueous solution, $C \sim 3\%$. The solvents were filtered with 0.2 μm size Millipore filter to remove possible dusts before being used to dilute the Nafion stock solution. It should be noted that although there is still a small amount of ethanol remaining in the stock solution, the percentage of ethanol in the final solution is negligible since the stock solution was typically diluted a few tens to few hundred times.

Dynamic Light Scattering (DLS). The light scattering measurements were carried out on a modified light scattering spectrometer (ALV/SP-125 with an ALV-5000 digital correlator). A solid-state laser (ADLAS DPY425, 400 mW at $\lambda = 532$ nm) was used as the light source. The incident beam was vertically polarized with respect to the scattering plane. All measurements were made at 25.0 ± 0.1 °C. The measured intensity−intensity time autocorrelation function $G^{(2)}(t,q)$ is related to the first-order electric field correlation function $|g^{(1)}(t,q)|$ by[26,27]

$$G^{(2)}(t,q) \equiv \langle I(0)\, I(t)\rangle = A[1 + \beta|g^{(1)}(t,q)|^2] \qquad (1)$$

where A is the measured baseline and β a constant of order unity which is a measure of detection coherence. The magnitude of the scattering wavevector $q = (4\pi n/\lambda_0)\sin(\theta/2)$ with n, λ_0, and θ being the solvent refractive index, the laser wavelength in a vacuum, and the scattering angle, respectively. For a dispersed system, $|g^{(1)}(t,q)|$ can be related to the normalized characteristic line width distribution $G(\Gamma)$ by

$$|g^{(1)}(t,q)| \equiv \langle E(0)\, E^*(t)\rangle = \int d\Gamma\, G(\Gamma)\exp(-\Gamma t) \qquad (2)$$

Using the Laplace inversion program CONTIN, $G(\Gamma)$ can be calculated from $G^{(2)}(t,q)$. Note that Γ is a function of both q and C. For a diffusive process, Γ can be expressed as[29,30]

$$\Gamma/q^2 = D(1 + k_d C)(1 + f\langle R_g^2\rangle q^2) \qquad (3)$$

where D is the translational diffusion coefficient at the limits of $C \to 0$ and $q \to 0$, k_d the diffusion second virial coefficient, R_g the radius of gyration, and f a measure of chain conformation and internal motion. Thus, a distribution of Γ, such as $G(\Gamma)$, can be converted to a diffusion coefficient distribution or to a hydrodynamic radius (R_h) distribution through $R_h = k_B T/(6\pi\eta D)$, where k_B and η are the Boltzmann constant and solvent viscosity, respectively. For very dilute solutions and with $\langle R_g\rangle q \ll 1$, as in our study, $D \cong \Gamma/q^2$. In the case of Nafion aqueous solutions without additives (glycerol or LiCl), multimodes are observed and sometimes cannot be resolved by the CONTIN program. In this case, we fitted the correlation function $G^{(1)}(t)$ with a triple-exponential function:

$$G^{(2)}(t) = 1 + A_1\exp(\Gamma_1 t) + A_2\exp(\Gamma_2 t) + A_3\exp(\Gamma_3 t) \qquad (4)$$

Results and Discussion

Figure 1 shows a few typical differential distribution curves $F(R_h)$ of the apparent hydrodynamic radius R_h, obtained from CONTIN analysis of the light scattering data for 5.31×10^{-3} g/mL Nafion in deionized water. These distributions show that there exist multimodes in Nafion/water system. At low angle, i.e., $\theta = 20°$, there are two peaks, ranging from 100 to 1000 nm. With increasing θ, these two peaks gradually merge into one that can no longer be resolved by CONTIN, whereas another peak, located at a few tens of nanometers, appears gradually. These types of multimodes are observed in all of the Nafion aqueous solutions measured, with concentrations varying from 1×10^{-4} to 5.3×10^{-3} g/mL. We label them as fast, medium, and slow modes, respectively. By fitting the correlation function with eq 4, the average line width (decay rate) Γ and the relative weight of each mode can be obtained. The corresponding size of a mode can also be obtained by converting the line width into an apparent hydrodynamic radius R_h. Table 1 shows the fitting results of the correlation functions measured at various scattering angles for a solution with Nafion concentration $C = 5.31$

Table 1. Triple-Exponential Fitting Results of Measured Correlation Functions from Nafion Aqueous Solutions of Polymer Concentration $C = 5.31 \times 10^{-3}$ g/mL

scattering angle (deg)	fast mode			medium mode			slow mode		
	Γ_f (ms^{-1})	$R_{h,f}$ (nm)	A_f (%)	Γ_m (ms^{-1})	$R_{h,m}$ (nm)	A_m (%)	Γ_s (ms^{-1})	$R_{h,s}$ (nm)	A_s (%)
20	0.64	13.6	0.52	0.04	212	56	0.105	818	44
30	1.16	16.5	0.7	0.12	161	35	0.034	560	64
60	1.25	57.5	0.8	0.31	226	49	0.098	728	49
90	5.43	26.4	2.7	1.05	136	28	0.27	530	70

Table 2. Triple-Exponential Fitting Results of Measured Correlation Functions from Nafion Aqueous Solutions of Concentration $C = 1.03 \times 10^{-3}$ g/mL

scattering angle (deg)	fast mode			medium mode			slow mode		
	Γ_f (ms^{-1})	$R_{h,f}$ (nm)	A_f (%)	Γ_m (ms^{-1})	$R_{h,m}$ (nm)	A_m (%)	Γ_s (ms^{-1})	$R_{h,s}$ (nm)	A_s (%)
20	0.81	10.6	0.49	0.052	166.4	54	0.0142	608	46
30	0.57	33.3	2.7	0.088	217	73	0.0214	896	24
60	1.64	43.5	4.2	0.46	154.4	45	0.14	506.1	51
90	2.6	53.6	16	0.43	331.3	84			

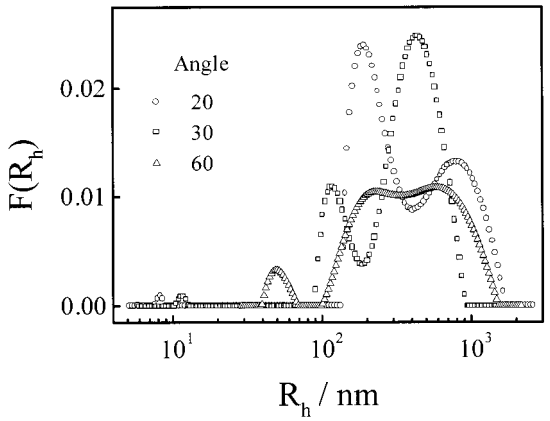

Figure 1. Differential distribution $F(R_h)$ of apparent hydrodynamic radius R_h in Nafion aqueous solutions measured at various scattering angles. The measurements were made at polymer concentration $C = 5.31 \times 10^{-3}$ g/mL and temperature $T = 25$ °C.

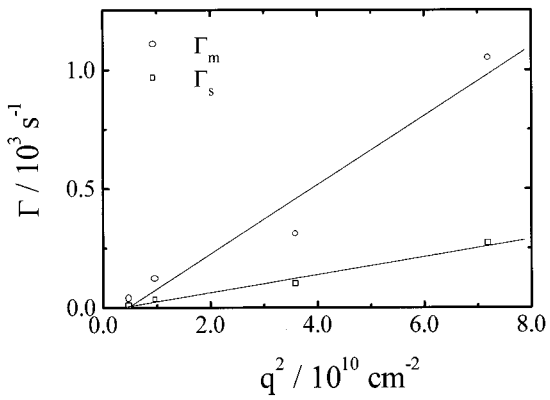

Figure 2. Typical q^2 dependence of the average line width Γ for the slow and medium modes of a Nafion aqueous solution with $C = 5.31 \times 10^{-3}$ g/mL.

$\times 10^{-3}$ g/mL. The subscripts in the table denote the fast, medium, and slow modes, respectively. Table 2 lists similar results for a solution with $C = 1.03 \times 10^{-3}$. In Figure 2 we plot the average line widths Γ_s and Γ_m as a function of q^2 for the slow and the medium modes, respectively ($C = 5.31 \times 10^{-3}$ g/mL). Although the data are somewhat scattered, the linear dependence of Γ on q^2 indicates that both modes are related to the translational diffusion of fast- and slow-moving species. As shown in Figure 3, approximate linear dependence on q^2 for the average line width Γ_f of the fast mode is also observed. This means that the fast mode is also related

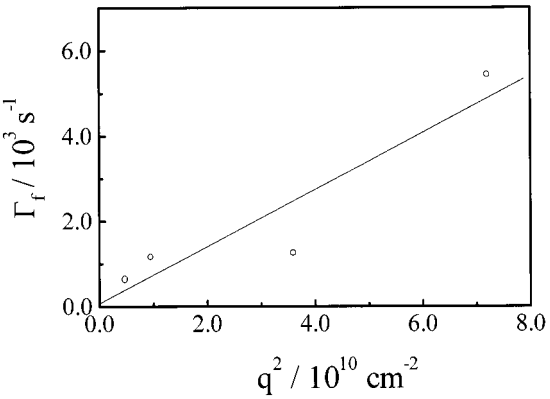

Figure 3. q^2 dependence of the average line width Γ for the fast mode in Nafion aqueous solution with $C = 5.31 \times 10^{-3}$ g/mL. The insert is the plot of the relative weight of this mode from the fitting vs q^2, where a_f (%) $= 100a_f/(a_f + a_m + a_s)$.

Table 3. Concentration Dependence of the Aggregates Size ($R_{h,m}$, $R_{h,s}$) and of the Corresponding Size ($R_{h,f}$) of the Internal Motion

C (g/mL)	$R_{h,f}$ (nm)	$R_{h,m}$ (nm)	$R_{h,s}$ (nm)
1.03×10^{-3}	35	179	670
5.31×10^{-3}	29	183	659

to a diffusion process. Note that the molecular mass of Nafion is about 2×10^5, which corresponds to a chain length of about 150 nm. The fact that the sizes corresponding to the slow and the medium modes are larger than the chain length of an individual polymer implies that both are related to Nafion aggregates. Table 3 shows the angle-averaged sizes of these two aggregates, together with the size corresponding to the fast mode, for the two concentrations of Tables 1 and 2. From the table, it is clear that the sizes of these aggregates show no apparent concentration dependence. If one assumes that there exists an equilibrium between individual Nafion chains and aggregates, one is then inclined to attribute the fast mode to the individual chains, since it is known that Nafion is molecularly dispersed in absolute ethanol solution. However, from the DLS measurement of a 1.3×10^{-3} g/mL Nafion/EtOH solution (in which no aggregate exists), we did not observe a decay rate that would correspond to the translational motion of individual Nafion chains. This implies that the refractive index contrast between the individual coils and the solvent (EtOH) is not large enough for DLS to measure the translational motion of the individual chains. Since ethanol and water have comparable refractive indices, the fast mode observed in the aqueous

Table 4. Apparent Hydrodynamic Radii ($R_{h,m}$) of the (Intrinsic) Nafion Aggregates, in nanometers, in Aqueous Solutions in the Presence of Salt (LiCl) and/or Glycerol (GL) for Different Polymer Concentrations C[a]

		scattering angle (deg)					
additive	C (g/mL)	20	30	45	60	90	average
GL	1×10^{-4}	113 (4.2)	119 (8.6)	110 (13.3)	93 (5.9)	84 (6.6)	104 (7.7)
GL	2×10^{-4}	160 (4.5)	145 (8.5)	138 (2.6)	127 (2.2)	117 (5.7)	137 (4.7)
GL	4×10^{-4}	168 (6.6)	158	138 (4.2)	130 (2.3)	121 (1.7)	143 (3.7)
LiCl	1.1×10^{-4}	242 (30)	235 (35)		173 (22)		217 (29)
GL + LiCl	1.6×10^{-4}	191	179	148	149	138	161

[a] Also shown are the sizes ($R_{h,f}$) corresponding to the internal motions of the aggregates (numbers in the parentheses).

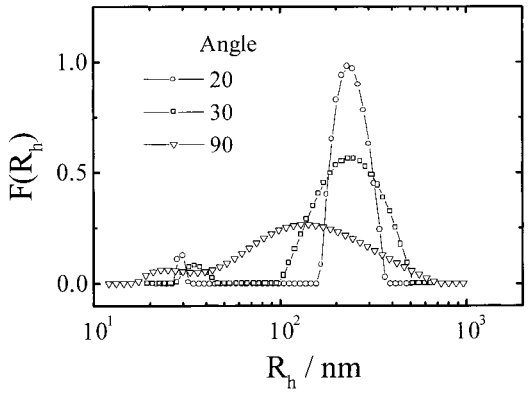

Figure 4. Differential distribution curves of 1.1×10^{-4} g/mL Nafion in aqueous solution with 0.5 M LiCl measured at various scattering angles, where the secondary aggregations are seen to be suppressed completely.

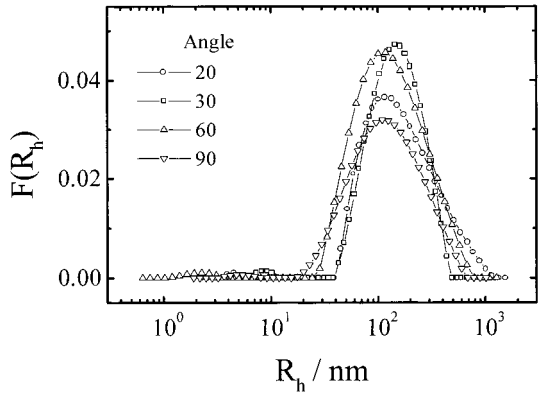

Figure 5. Differential distribution $F(R_h)$ of 2.0×10^{-4} g/mL Nafion in aqueous solution with 5% glycerol measured at various scattering angles. It is seen that the secondary aggregations are completely suppressed.

Nafion solutions cannot come from the individual Nafion chains. To confirm this, we filtered a Nafion aqueous solution with a 200 nm filter. Since the pore size of the filter is smaller than the sizes of both aggregates, they would be removed from the solution during filtration while individual chains should pass through the filter. After filtration, however, nothing remained inside the solution; the intensity of the scattering light dropped to the same level as that of pure deionized water. Therefore, the fast mode should not be the translational diffusion of the individual Nafion chains, but rather associated with the internal motion of Nafion aggregates (the nature of this "internal motion" will be discussed below). The existence of the dominating twin peaks indicate that in aqueous solution Nafion must be engaged in more than one form of association, which leads to the dual sized aggregates.

To investigate the origins of the aggregates, we add salt LiCl to aqueous Nafion solutions. Figure 4 shows the apparent size distribution in a 1.1×10^{-4} g/mL Nafion aqueous solution with 0.5 M LiCl. Here we see clearly that the larger (secondary) aggregates are suppressed by the addition of LiCl, suggesting that these aggregates form via electrostatic interactions. The electrostatic interactions may originate from the attraction between nonionized ion pairs, which can be suppressed in the environment of high ionic strength. Figure 5 shows the apparent size distribution of 2.0×10^{-4} g/mL Nafion in 5% glycerol aqueous solutions measured at various scattering angles. Similar to the LiCl aqueous solution case, the larger peak of the dominating dual peaks observed in Nafion aqueous solutions without additives is suppressed here. The suppression can also be confirmed by fitting the correlation function with eq 4, with the result showing that there exists only one exponential term in the 100−1000 nm range. Table 4 lists the sizes of the (intrinsic) Nafion aggregates ($R_{h,m}$) in 5% glycerol, 0.5 M LiCl, and the mixture of 5% glycerol and 0.5 M LiCl. Also shown in the table are the apparent hydrodynamic sizes corresponding to the internal motions (numbers in parentheses). Combining Tables 3 and 4, we see that the addition of glycerol not only suppresses the secondary aggregation but also decreases the size of the intrinsic Nafion aggregates. While the size of the aggregates show no significant concentration dependence in aqueous solutions without additives, we see from Table 4 that it increases with Nafion concentration in solutions with 5% glycerol. With increasing Nafion concentration, the size corresponding to the internal motions also shifts to smaller scales. From Table 4, we see that the addition of LiCl will cause the increase of the intrinsic aggregate size. This increase can be explained by the screening of the polyelectrolyte effect, i.e., the electrostatic repulsion (see below). On the basis of the above results, we obtain the following picture for Nafion aqueous solutions: (1) due to hydrophobic interactions with water, most Nafion chains associate with each other to form (relatively large) aggregates, with hydrodynamic radii varying from 100 to 200 nm, which will be called intrinsic aggregates; (2) the intrinsic aggregates can further interconnect through nonionized ion pairs to form a secondary (or higher level) aggregation, the hydrodynamic radii of these larger aggregates range from 500 to 800 nm; (3) the intrinsic aggregates have internal motions with corresponding sizes of a few to few tens of nanometers; and (4) the addition of either salt or glycerol suppresses the secondary aggregation.

We investigate now the nature of the aggregates. A "rodlike" structure for Nafion molecules in solution has been suggested in the literature on the basis of the SAXS and SANS spectra of dilute solutions.[19,20] Conductivity, ESR, and ^{19}F NMR data further confirmed the validity of the rodlike model. In the model, the perfluoro backbone constitutes the solvophobic core of the rod, the pendant chains are located at the periphery

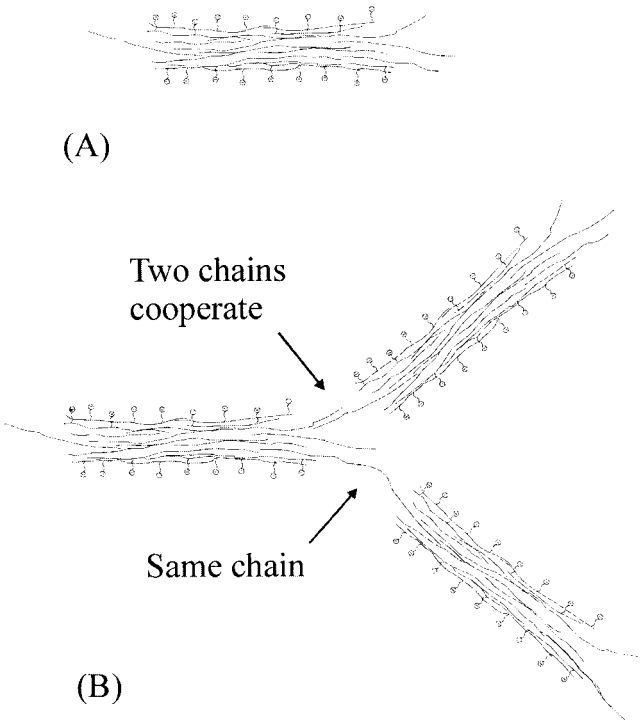

Figure 6. Schematics of (a) the fringed-rod model (taken from ref 24) and (b) fringed-rod-based microgel model, which shows a cross-linking mechanism between fringed rods inside an intrinsic Nafion aggregate.

of the rods, and the ionic groups are around the surface of the rod like fringes. The rod radius is determined to be about 2.4 nm with an estimated persistence length of about 40 nm based on SANS and SAXS data.[19,20] In the meantime, on the basis of the electron spin resonance study of Nafion solutions and swelling membranes, Szajdzinska-Pietek et al. used the fringed-rod model to describe the morphology of Nafion aggregates in solutions, which is shown in Figure 6a.[24] Their basic assumption[24] was that at low ionomer concentrations only part of the chain segments are incorporated into a rod, and other segments are outside the rods. As the concentration of the polymer increases, parts of the chains "dangling" outside of the rods become incorporated into other rods.[24] It should be noted that the concentration range used in our experiments is between 1×10^{-4} and 1×10^{-3} g/mL in most cases, which is much lower than the minimum concentration, 1×10^{-2} g/mL, used in the ESR experiment. Our light scattering results indicate that even at low Nafion concentrations, the isolated rod cannot exist in stable form due to the strong hydrophobic effect of Nafion backbone. Therefore, we propose a model of a Nafion microgel cross-linked through the solvophobic interaction of Nafion backbone. Figure 6b shows schematically two types of joints that connect different fringed rods in one aggregate or microgel. In this fringed-rod based model, one or several Nafion chains form fringed rods which further interconnect with each other through the incorporation of the dangling chain segments at their ends to form large Nafion aggregates. These secondary aggregates may be viewed as Nafion microgels since some of the dangling chain joints connect more than two rodlike units, acting as cross-linking points.

On the basis of this microgel model, we now discuss the effect of adding salt or glycerol to Nafion solutions. The structures of ionomer solutions are known to be governed by both the polarity of the solvent and solubility of the polymer backbone.[31] Due to the similar properties between glycerol and ethanol, the perfluoro backbone of Nafion is expected to have a higher solubility in glycerol. Therefore, the addition of a small amount of glycerol will cause Nafion to become more solvated, and some glycerol molecules may even penetrate into Nafion backbone, which will cause a decrease of the elastic energy, leading to the decrease of the radius and the persistence length of the rod. The fact that only aggregates of around a few hundreds nanometers in size are observed after addition of the glycerol (Figure 5) indicates that the increased solvated effect limits the higher level aggregation. Also, the increased solvated effect will make part of the rod joint (the self-assembled dangling chains) dissociate so that the size of Nafion aggregates decreases. In many physically cross-linked or chemically cross-linked microgel and bulk gel systems, a diffusive fast mode is often observed by DLS. This fast mode can be attributed to the relative motion between two neighboring cross-linked points. Thus, on the basis of our microgel model for Nafion solutions, we may attribute the fast mode observed by DLS to the associated rod motion between two neighboring cross-linking points. For Nafion aqueous solutions without additives, triple-exponential fitting was used to obtain the characteristic times of the dual sized Nafion aggregation and the internal motion. Because of the tiny fraction of the internal motion in the overall signal, such multiparameter fitting cannot give the exact value for the decay rate of the internal motion. Nevertheless, we can still find qualitatively that the addition of glycerol increases the decay rate (or decreases the corresponding length) of the internal motion, indicating increased mobility of Nafion rod segment due to the increased solvated effect.

Similar to the glycerol case, the addition of salt also suppresses the secondary level aggregation. The dual sized aggregates observed in aqueous solutions without any additives imply that there are two types of driving forces that are responsible for aggregation. Beside the solvophobic interaction, which is responsible for the initial (or intrinsic) aggregation, further (or secondary) aggregation may occur between these aggregates through the electrostatic attraction between nonionized ion pairs on the solvated backbone.[32] This electrostatic attraction can be effectively screened by the addition of counterions.

The existence of the large (secondary) Nafion aggregates is possibly due to the different polymer concentrations used in our measurements and in those of others. Light scattering is especially sensitive to large aggregates, which allows us to study Nafion solutions of much lower concentration than that required by the methods of SANS, SAXS, and ESR. The overlap concentration, C^*, of Nafion aggregates can be roughly estimated from its mass M_w and radius of gyration R_g, using $C^* = 3M_w/(4\pi N_A R_g^3)$, where N_A is Avogadro's number. For Nafion aqueous solutions, C^* is about 1.2×10^{-3} g/mL. When the concentration is higher than C^*, the Nafion aggregates come into contact with, or even penetrate inside, each other. Since SANS and SAXS are based on Bragg diffraction, it is reasonable that aggregates of this dimension cannot be observed by SANS and SAXS when Nafion concentrations are higher than the overlap concentration. In Nafion/EtOH solution, no aggregate was observed. This result is consistent with

the ESR result, while SANS and SAXS still observed Nafion colloidal structure. Considering a rod which contains only one Nafion chain, on the basis of density = 2.07 g/mL and radius = 2.0 nm (in ethanol solution) and molecular mass = 2×10^5 g/mol, its length is ~14 nm. On the basis of this, we speculate that the colloidal structures observed by SANS and SAXS measurements are the single-chain Nafion micelles, not Nafion aggregates.

Moreover, we have reached some different results from that of Cirkel et al.:[28] we found three R_h peaks in aqueous solution, instead of one; we found no peak in ethanol solution, rather than two. These might change the current understanding that there was no qualitative difference for various Nafion solutions. In addition, our finding of the suppression of larger R_h reveals the origin of the ionic conductivity drop, which is critical to the application in fuel cells.

Conclusion

In this paper, we report dynamic light scattering study of the self-assembling behavior in Nafion aqueous solutions. Two kinds of aggregates are found. One is an intrinsic aggregate (~150 nm) due to the hydrophobic interaction of fluorocarbon backbone, which is found to be always present in aqueous solution. The other is a larger, secondary aggregate, which can be suppressed by the addition of salt or a small amount of glycerol. A fringed-rod-based microgel model for aqueous Nafion solutions is proposed, in which one or several Nafion chains form fringed rods that further interconnect with each other through the incorporation of the dangling chain segments at their ends to form large Nafion aggregates. These secondary aggregates may be viewed as Nafion microgels since some of the dangling chain joints connect more than two rodlike units, acting as cross-linking points. With the proposed microgel model, we are able to explain the observed suppression of the secondary aggregation by the addition of salt or glycerol.

The results of our study will be useful to the understanding of ion cluster formations in the casting of Nafion membranes from solutions. High ion conductivity requires large ion clusters and ion connection between ion clusters. In our view, the further aggregation, which is governed by the nonionized ion pairs, may provide the ion connection between the ion clusters or facilitate the formation of large ion clusters in recast membrane.

Acknowledgment. We thank Prof. Chi Wu for helpful discussions and generous loan of his light scattering apparatus. We gratefully acknowledge support of this work by the Research Grants Council of the Hong Kong Special Administrative Region through a Direct Grant for Research (Project ID 2060136). G.X. expresses his sincere gratitude for the C.N. Yang Visiting Fellowship from, and the hospitality of, the Physics Department of the Chinese University of Hong Kong during Nov−Dec 1998.

References and Notes

(1) Eisenberg, A., Yeager, H. L., Eds. *Perfluorinated Ionomer Membranes*; ACS Symposium Series 180; American Chemical Society: Washington, DC, 1982.
(2) Yeo, R. S.; Chin, D. T. *J. Electrochem. Soc.* **1980**, *127*, 546.
(3) Appleby, A. J., Foulkes, R. L., Eds. *Fuel Cell Handbook*; Van Nostrand: New York, 1989.
(4) Wilson, M. S.; Gottesfeld, S. *J. Appl. Electrochem.* **1992**, *22*, 1.
(5) Ren, X. M.; Wilson, M. S.; Gottesfeld, S. *J. Eletrochem. Soc.* **1996**, *143*, L12.
(6) Zaluski, C.; Xu, G. *Macromolecules* **1994**, *27*, 6750.
(7) Gierke, T. D.; Munn, G. E.; Wilson, F. C. *J. Polym. Sci., Polym. Phys. Ed.* **1981**, *19*, 1687.
(8) Starkweather, H. W. *Macromolecules* **1982**, *15*, 320.
(9) Fujimura, M.; Hashimoto, T.; Kawai, H. *Macromolecules* **1981**, *14*, 1309.
(10) Moore, R. B.; Martin, C. R. *Macromolecules* **1989**, *22*, 3594.
(11) Eisenberg, A.; Hird, B.; Moore, R. B. *Macromolecules* **1990**, *23*, 4098.
(12) Zaluski, C.; Xu, G. *J. Electrochem. Soc.* **1994**, *141*, 448.
(13) Xu, G.; Park, Y. S. *J. Electrochem. Soc.* **1992**, *139*, 2871.
(14) Martin, C. R.; Rhoades, T. A.; Ferguson, J. A. *Anal. Chem.* **1982**, *54*, 1639.
(15) Moore, R. B.; Martin, C. R. *Macromolecules* **1988**, *21*, 1334.
(16) Arimura, T.; Ostrovskii, D.; Okada, T.; Xie, G. *Solid State Ionics* **1999**, *118*, 1.
(17) Otsuki, S.; Adachi, K. *J. Appl. Polym. Sci.* **1995**, *56*, 697.
(18) Sabatani, E.; Nikol, H. D.; Gray, H. B.; Anson, F. C. *J. Am. Chem. Soc.* **1996**, *118*, 1158.
(19) Aldebert, P.; Dreyfus, B.; Pineri, M. *Macromolecules* **1986**, *19*, 2651.
(20) Williams, C. E. *J. Phys. Chem. B* **1997**, *101*, 1884.
(21) Loppinet, B.; Gebel, G. *Langmuir* **1998**, *14*, 1977.
(22) Szajdzinska-Pietek, E.; Schlick, S.; Plonka, A. *Langmuir* **1994**, *10*, 1101.
(23) Szajdzinska-Pietek, E.; Pilar, J.; Schlick, S. *J. Phys. Chem.* **1995**, *99*, 313.
(24) Szajdzinska-Pietek, E.; Schlick, S.; Plonka, A. *Langmuir* **1994**, *10*, 2188.
(25) Gebel, G.; Loppinet, B. *J. Phys. Chem. B* **1997**, *101*, 3980.
(26) Chu, B. *Laser Light Scattering*, 2nd ed.; Academic Press: New York, 1974.
(27) Pecora, R.; Berne, B. J. *Dynamic Light Scattering*; Plenum Press: New York, 1976.
(28) Cirkel, P. A.; Okada, T.; Kinugasa, S. *Macromolecules* **1999**, *32*, 531.
(29) Stockmayer, W. H.; Schmidt, M. *Pure Appl. Chem.* **1982**, *54*, 407.
(30) Stockmayer, W. H.; Schmidt, M. *Macromolecules* **1984**, *17*, 509.
(31) Gebel, G. In *Macromolecular Complexes in Chemistry and Biology;* Dubin, P., Bock, J., Davies, R. M., Schulz, D. N., Thies, C., Eds.; Springer-Verlag: Heidelberg, 1994; Chapter 19, p 329.
(32) Wu, C.; Woo, K.; Jiang, M. *Macromolecules* **1996**, *29*, 5361.

MA010124B